

RESEARCH

Open Access



Observation of antitumor mechanism of GE11-modified paclitaxel and curcumin liposomes based on cellular morphology changes

Hailing Tang^{1,2*} , Lijuan Li³, Baoshan Wang⁴ and Guangxi Scientific Research Center of Traditional Chinese Medicine⁵

Abstract

Curcumin and paclitaxel are widely used as anti-tumor hydrophobic model drugs for the designation of smart tumor-targeting nanocarriers and the study of the correlation between structural characteristics of nanoparticles and in vivo therapeutic efficacy. Various signaling pathways on cell growth and proliferation have been comprehensively studied in vitro and in vivo under the action of curcumin and paclitaxel nanoparticles. In this paper, we prepared EGFR-targeted GE11 peptide-modified curcumin and paclitaxel compound liposomes (CUR-PTX@GE11-L). The tumor suppression mechanism of CUR-PTX@GE11-L is observed from the aspects of drug release behavior, changes of cell morphology, liver retention, and tumor-targeting efficiency. We hope it can provide a new vision for the rational construction of smart nanoscale drug delivery system through the observation of cytotoxic effects of CUR-PTX@GE11-L, especially on the cellular morphology change.

Keywords EGFR targeting, Cytotoxic effect, GE11 peptide, Paclitaxel, Curcumin

*Correspondence:

Hailing Tang
hltang2010@163.com

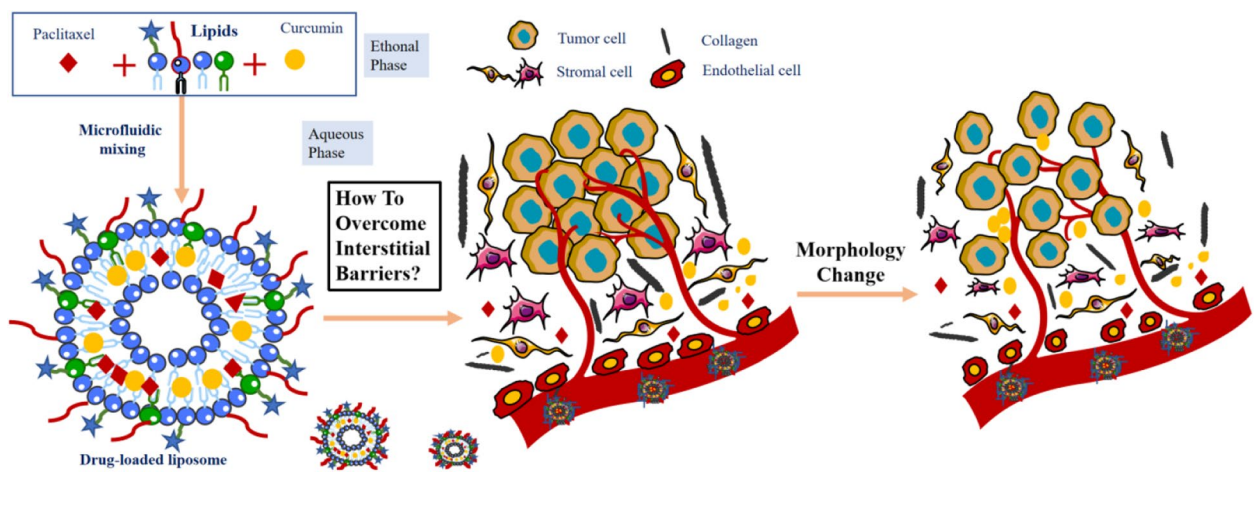
Full list of author information is available at the end of the article



© The Author(s) 2024. **Open Access** This article is licensed under a Creative Commons Attribution 4.0 International License, which permits use, sharing, adaptation, distribution and reproduction in any medium or format, as long as you give appropriate credit to the original author(s) and the source, provide a link to the Creative Commons licence, and indicate if changes were made. The images or other third party material in this article are included in the article's Creative Commons licence, unless indicated otherwise in a credit line to the material. If material is not included in the article's Creative Commons licence and your intended use is not permitted by statutory regulation or exceeds the permitted use, you will need to obtain permission directly from the copyright holder. To view a copy of this licence, visit <http://creativecommons.org/licenses/by/4.0/>.

Graphical Abstract

Changes of morphology and spatial structure of stromal cells and components on intra-tumoral diffusion and penetration of lipid nanocarriers after the administration of lipid nanocarriers.



Introduction

Liposome is the earliest successful nanodrug delivery carrier system in clinical application formed by amphiphilic phospholipid bilayers (Barenholz 2012). So far, more than 20 liposomal drugs have been approved for marketing in worldwide (Wang et al. 2019a, b). Liposomal Vyxeos developed by Celator is the only liposomal drug granted as a breakthrough therapy by FDA in August 2017, loading with daunorubicin and cytarabine (5:1 molar ratio) for the treatment of acute myeloid leukemia (Cortes et al. 2022). Compared with standard cytarabine and daunorubicin (7+3) therapy, the clinical profit of the compound liposome is obvious due to reducing clinical risks when the two drugs were administrated alone. The successful marketing of daunorubicin/cytarabine compound liposomes (Vyxeos) has attracted more and more attention for the development of novel compound liposomes (Blair 2018).

As early as the 1870s, Bangham conducted detailed studies on the distribution characteristics of encapsulated active molecules in the bilayer of phospholipid membranes and their effects on the structural stability of phospholipid membranes (Yamamoto and Bangham 1978). Paclitaxel (PTX) is a representative taxane drug for the chemotherapy of ovarian cancer, cervical cancer, breast cancer, and other cancers with obvious clinical anti-cancer effect (Zhang et al. 2022). At present, some paclitaxel injections, including paclitaxel albumin (Abraxane[®]), Taxol[®], and paclitaxel liposomes (Lipusu[®]), can be obtained in market. However, with the increased

resistance of tumor cells against cytotoxic drugs, the therapeutical outcome of PTX is also affected (Liu et al. 2016). Meanwhile, PTX is also accompanied by a series of toxic adverse effects, such as neurotoxicity (Caillaud et al. 2022), hepatotoxicity (Gur et al. 2022), and cardiotoxicity (Khaled et al. 2022). How to overcome the clinical use risks of PTX is a major problem that needs to be solved to improve the anti-cancer efficacy and safety of PTX (Ashrafizadeh et al. 2020). Curcumin (CUR) is an active monomer component of natural medicine with multi-target effects, which exhibited various therapeutic effect on tumor, inflammatory, diabetes, and so on (El-Saadony et al. 2022). Studies have shown that CUR can enhance antitumor efficiency of PTX (Saghatelian et al. 2020). It can downregulate the expression of P-gp, PKC- α , Bcl-2, MPP-9, GSK-3, ABCG-2, IKB- α , NF- κ B, PI3KCA, NF- κ B-snail, e-cadherin, N-cadherin, and other signaling pathway proteins or membrane proteins (Liu et al. 2022; Aggarwal et al. 2005). At the same time, the expression of Bax, Caspase-3, P53, PK38 MAPK, and other signaling pathways was upregulated (Dang et al. 2015).

CUR and PTX are both insoluble drugs. Many nanocarrier systems such as graphene oxide (Muthoosamy et al. 2016), polymer nanoparticles (Wang et al. 2016), lipid nanoparticles (Jiang et al. 2018), and gold nanoparticles (Zhu et al. 2019) can be used for simultaneous encapsulation and co-delivery of CUR and PTX. Among them, based on the safety of phospholipid excipients, compound liposomes loaded with CUR and PTX shows a great prospect for clinical application. Kaiqiu Jiang et al.

(2018) prepared RGD-modified CUR-PTX compound liposomes by thin film dispersion method, which significantly inhibited the tumor growth in human lung adenocarcinoma cell (A549 cell) tumor-bearing mouse model, and reflected the synergistic effect of CUR and PTX by MTT assay. RGD-modified CUR-PTX liposomes showed a prolonged in vivo half-life of PK parameters of CUR and PTX and a faster in vitro release behavior of PTX comparing to CUR.

In previous studies, lipid prescription was optimized by using Box-Behnken effect-response surface method to obtain the optimal lipid prescription range, which can achieve stable liposomal encapsulation of curcumin and paclitaxel (H T et al 2021). In this study, EGFR-targeted dodecapeptide GE11 (YHWYGYTPQNVI) screened by phage display peptide library was modified on the surface of liposome to prepare GE11-modified curcumin and paclitaxel compound liposome (CUR-PTX@GE11-L) (Tang et al. 2014). CUR-PTX@GE11-L were prepared by microfluidic chip technology (Hamano et al. 2019). The key quality properties of CUR-PTX@GE11-L modified with different surface densities of DSPE-MPEG-GE11, such as particle size, morphology, encapsulation rate, and release rate, were determined. The in vivo targeting efficiency and cytotoxic effect of CUR-PTX@GE11-L were also investigated.

Materials

Egg yolk phosphatidylcholine (EPC) was a gift from Guangzhou Baiyunshan Hanfang Pharmaceutical Co., Ltd. Cholesterol (CHOL), and 1,2-distearoyl-sn-glycero-3-phosphoethanolamine-N-methoxyl-(polyethylene glycol)-2000 (DSPE-PEG2000) were purchased by AVT (Shanghai) Pharmaceutical Technology Co., Ltd. 1,2-Distearoyl-sn-glycero-3-phosphoethanolamine-N-maleimide-(polyethylene glycol)-2000-GE11 (DSPE-PEG2000-GE11) was purchased from Xi'an Ruixi Biotechnology Co., Ltd. Anhydrous ethanol was purchased by Chengdu Cologne Chemicals Co., Ltd. Sodium chloride was from Tianjin Zhiyuan Chemical Reagent Co., Ltd. Lipophilic fluorescent dye DID was from AAT

Bioquest (USA). Curcumin and paclitaxel were supplied by Shanghai Aladdin Biochemical Technology Co., Ltd. The 300 mesh copper carbon film was purchased from Suzhou Crystal Silicon Electronic & Technology Co., Ltd. Paclitaxel liposomes (Lipusu[®]) were supplied from Shandong Luye Pharma. All other reagents were of chemical pure or analytical grade from Sinopharm Chemical Reagent Co. Ltd. (Shanghai, China).

Methods

Preparation of CUR-PTX@GE11-L

Liposome samples were prepared by a one-step method using microfluidic chip technology. Ethanol lipid reserve solutions of 240 mg/mL EPC, 20 mg/mL CHOL, 120 mg/mL DSPE-PEG2000, 60 mg/mL DSPE-PEG2000-GE11, 20 mg/mL CUR, and 20 mg/mL PTX were prepared, separately. Ethanol lipid phase was prepared according to the lipid formulation of CUR-PTX@GE11-L, as Table 1 shows.

Liposome samples were prepared by INano rapid nanopreparator (iNano Lab System, Maianna (Shanghai) Instrument Technology Co., Ltd.). Preparation parameters were set as follows: 20 mL/min was the total flow rate, 1:9 was the volume ratio of ethanol phase to aqueous phase, and 8 mL was the total flow volume. Using 5% glucose as aqueous phase, the obtained liposome samples were removed by rotary evaporator (EYELA, TOKYO RIKAKIKAI Co., Ltd) and stored at 4 °C.

CUR-PTX@GE11-L were prepared by two-steps. Firstly, curcumin and paclitaxel liposomes (CUR-PTX@L), DSPE-PEG2000 micelles, and DSPE-PEG2000/DSPE-PEG2000-GE11 mixed micelles were prepared respectively. Secondly, CUR-PTX@L and DSPE-PEG 2000 micelles or DSPE-PEG2000/DSPE-PEG2000-GE11 mixed micelles were mixed using the INano rapid nanopreparator. The preparation parameters were set as follows: 5 mL/min was the total flow rate, and 1:1 was the volume ratio of the liposomes phase to the micellar phase. PEG-modified curcumin and paclitaxel liposomes (CUR-PTX@PEG-L) and PEG/GE11-modified curcumin

Table 1 Lipid formulation of CUR-PTX@GE11-L

	EPC (mM)	CHOL (mM)	DSPE-MPEG (mM)	DSPE-MPEG-GE11 (mM)	CUR (mM)	PTX (mM)
DSPE-MPEG micelle	0	0	4.2	0	0	0
DSPE-MPEG-GE11 micelle	0	0	3.2	0.67	0	0
CUR@L	155.8	15.5	0	0	8.1	0
CUR-PTX@PEG-L	155.8	15.5	4.2	0	4.1	1.8
CUR-PTX@GE11-L	155.8	15.5	3.2	0.67	4.1	1.8

and paclitaxel liposomes (CUR-PTX@GE11-L) were prepared. For preparation of fluorescence liposomes, an addition of 20 μ L DID fluorescence dye (50 μ M) was added into 1 mL of lipid ethanol solution separately.

Determination of CUR and PTX by HPLC

Accurately weigh the appropriate amount of curcumin and paclitaxel substance to prepare curcumin and paclitaxel standard stock solution with ethanol. The stock solution of curcumin and paclitaxel were diluted at multiple ratios respectively for HPLC detection (Agilent 1200, USA). One hundred microliters of CUR-PTX liposome was added to 900 μ L isopropyl alcohol and centrifuged for 5 min at 5000 rpm. Then, 10 μ L supernate was directly injected for HPLC determination of CUR and PTX. Phenomenex Luna@5 μ m PFP 100 Å column (250 mm \times 4.6 mm) is employed. Acetonitrile (A) and 0.1% acetic acid solution (B) were consisted of the mobile phase. Sixty percent of acetonitrile (A) with a flow rate of 1 mL/min was used for isometric elution for 15 min. The detection wavelength is 227 nm, and chromatography column temperature is 30 °C. Both CUR and PTX have good specificity, and the precision of CUR and PTX was 1.6% and 0.2%, respectively, which meet the testing requirements. The peak area was drawn with the ordinate (Y) and the drug concentration (X) as the transverse ordinate. The standard curve equation of paclitaxel was $Y=18804X+40.976$ ($R^2=0.9994$), and the standard curve equation of curcumin was $Y=20744X+48.692$ ($R^2=0.9992$).

Encapsulation rate of CUR and PTX in liposomes

Before sample preparation, the liposome sample was restored to room temperature. One milliliter of liposome samples was centrifuged at 5000 rpm for 5 min, and 100 μ L supernatant was taken as test solution. Nine hundred microliters of isopropyl alcohol was then added for vortex demulsification. One hundred microliters of liposome samples were directly added with 900 μ L isopropyl alcohol as control solution after vortex demulsification. The treated sample solution were stored at 4 °C for unified testing. The encapsulation rate of CUR and PTX were $96.8 \pm 4.1\%$ and $95.5 \pm 1\%$, respectively.

In vitro release of CUR-PTX@GE11-L

Five milliliters of the prepared CUR-PTX@GE11-L samples were taken and adjusted to 25 mL at pH 7.4 phosphate buffer solution (PBS) (Jiang et al. 2018). Five milliliters of diluted samples were transferred to MW10000 dialysis bags, which were then placed in 900 mL release medium (pH 7.4 PBS) instead of 50% ethanol and stirred at 37 °C for 2 h, 4 h, 8 h, and 24 h, respectively. The concentration of CUR and PTX

was determined by HPLC as shown above, and the release behavior of CUR-PTX@GE11-L in vitro was investigated.

Morphology observation of CUR-PTX@GE11-L

Signal particle tracking technique (ZetaView, PARTICLEMETRIX, Germany) was applied to determine the particle size characteristics of liposome samples. Electron frozen transmission electron microscopy was used to observe the morphology of liposomes. Liquid nitrogen was added into the rapid freezing sample preparation device. When the temperature of ethane cooling cup dropped to -170 °C, the gaseous ethane was passed until the formation of liquid ethane. During the process, the air humidity was reduced to the minimum, and liquid nitrogen was prevented from splashing into the liquid ethane. Hydrophilic treatment was carried out on the copper mesh after microscopic examination. An appropriate amount of 4.5 μ L liposome sample was taken on the copper net and printed for 2 s on one side. The sample was frozen by liquid ethane and stored in the TEM sample box cooled by liquid nitrogen for later use. The samples were observed by field emission frozen transmission electron microscopy (Talos F200C G2, Thermo Fisher Scientific, USA) with a voltage of 200 KV. Take 4 to 5 cryo-TEM images for each sample to observe the number and percentage of non-spherical or multilayered liposomes.

Inhibition of proliferation and migration of HUVEC cells

Human umbilical vein endothelial cells (HUVEC) were inoculated into six-well plates and cultured to about 70% confluence using DMEM medium containing 10% FBS. Scratches were performed on monolayer cells, washed with PBS, and the scratched cells were removed. The liposome samples of 50 μ L CUR@L, CUR-PTX@PEG-L, and CUR-PTX@GE11-L were added and evenly dispersed in 5 mL DMEM medium containing 10% FBS, respectively. The cell proliferation and migration status before and after treatment with different liposome samples were observed by living cell workstation (Axio Observer7, ZEISS, Germany).

Proliferation inhibition of bone marrow stem cells (BMSC)

SD rats at 2 weeks of age were taken and sacrificed by cervical vertebrae dislocated. The femur and tibia of the rats were separated with sterilized tweezers and scissors under sterile conditions. The femur and tibia of the rats were cut in the middle, and bone marrow cells was sucked out with DEME solution by a 2-mL sterile syringe. After centrifugation at 1000 rpm for 5 min, the supernatant was discarded, and the cells was re-suspended with PBS. The cell suspension was slowly added

into a 15-mL centrifuged tube with 5 mL lymphocyte separation solution and kept on the upper layer. Then, the cell suspension was centrifuged at 2000 rpm for 20 min, and the middle layer with bone marrow stem cells (white and turbid) was sucked and washed three times with PBS. DMEM/F12 containing 15% FBS was used as culture medium. 10^6 /mL BMSC was inoculated into six-well culture plates and incubated in culture medium at 37 °C and 5% CO₂. After 24 h, the culture medium was discarded, and the non-adherent cells were rinsed with PBS for 2~3 times, and the culture medium was added for continued culture. Then, the third generation were taken to observe the inhibitory effect of curcumin and paclitaxel liposomes on the proliferation of BMSC. The liposome samples of 50 µL CUR@L, CUR-PTX@PEG-L, and CUR-PTX@GE11-L were added and evenly dispersed in 5 mL DMEM medium containing 10% FBS, respectively. The cell morphology status before and after treatment by liposome samples were observed after 5 µM calcein staining (DMi8, LEIKA, Germany).

Targeting efficiency of CUR-PTX@GE11-L in subcutaneous SMMC7721 xenografts

6×10^5 SMMC7721 cells containing 10 mg/ml MitroGel were injected subcutaneously in the right axils of nude mice aged 6~8 weeks. Mice were divided into 3 groups: the control group, CUR-PTX@PEG-L group, and CUR-PTX@GE11-L group. Each group has 3 mice. After inoculation for 2 weeks, the tumor diameters reached about 4~6 mm. CUR-PTX@GE11-L samples were injected caudally into mice at the dosage of 1.2 mg/kg PTX every 3 days for three times. In order to observe the distribution behavior and tumor target efficiency of CUR-PTX@GE11-L and CUR-PTX@PEG-L, DID-labeled CUR-PTX@GE11-L and CUR-PTX@PEG-L were injected intravenously into SMMC7721 subcutaneous xenografts respectively. In vivo fluorescence imaging system (IVIS Lumina XRMS III, Perkin Elmer, USA) was used to record the total fluorescence signal of tumor-bearing mice and the fluorescence signal values of tumor, the liver, and other major organs. All the animal experimental procedures were approved by the Animal Care and Use Subcommittee at Guangxi University of Chinese Medicine and performed according to Institutional Guidelines.

Results

Characterization of CUR-PTX@GE11-L

A two-step method to prepare CUR-PTX@GE11-L samples was used. Firstly, curcumin and paclitaxel liposomes without PEG/GE11 modification, DSPE-MPEG micelles, and DSPE-MPEG/DSPE-MPEG-GE11

micelles were prepared by microfluidic chip technology, respectively. Then, DSPE-MPEG/DSPE-MPEG-GE11 micelles were modified on the surface of curcumin and paclitaxel liposomes, using microfluidic chip technology. The construction and size control of liposomes are completely dependent on the process parameters and the lipid formulation, because a liposome extruder for the further adjustment of the particle size distribution was not applied. The particle size, morphology, and release behavior of encapsulated drugs of prepared liposome samples were well investigated as shown in Figs. 1 and 2.

The Cryo-TEM images of CUR@L, CUR-PTX@PEG-L, and CUR-PTX@GE11-L are exhibited in Fig. 1B, C, and D. The liposomes samples with three different formulations were almost monolayer liposomes, which also indicated that the microfluidic chip technology could effectively prepare monolayer liposomes. The manufacture efficiency, including the time cost and the sample loss rate, was obviously improved comparing to the traditional thin film hydration method for liposome preparation.

In the liposome preparation process, ethanol was removed by rotary evaporation apparatus under low vacuum and low temperature, which avoided the loss of lipid components and the precipitation of drugs happened in the process of ultrafiltration dialysis. The morphological characteristics of CUR-PTX@PEG-L and CUR-PTX@GE11-L were observed by cryo-TEM, and the morphological difference of these two liposome samples was compared and analyzed. CUR-PTX@GE11-L is a round and completely closed vesicle. Occasionally, the multi-layered structure or irregular bilayer morphology of vesicular liposome can be seen, as the arrows show in Fig. 2 (Table 2). The multi-layered vesicular liposome may be induced by the overlap of two liposomes at the time of filming, while the changes of the curvature of the lipid membrane are due to the insertion of curcumin and paclitaxel. During the process of ethanol removal by rotary evaporation, the occasional bubble appears, resulting in the rupture and fusion of the lipid membrane among liposomes. At the same time, we also used ZetaView (PARTICLE METRIX, Germany) to measure the particle size distribution of CUR@L, CUR-PTX@PEG-L, and CUR-PTX@GE11-L by single-particle tracking technique. The average size of each sample was 191.1 nm, 199.4 nm, and 165.6 nm, respectively, as Fig. 2G, H, and I shows. This irregular particle shape may influence the plasma protein adsorption and macrophage uptake behavior (Gao and He 2014).

The release behavior of curcumin and paclitaxel encapsulated in liposome directly affects the therapeutic effect of the preparation. The in vitro release of paclitaxel and curcumin liposomes in three groups with different prescriptions was investigated. At 2 h, curcumin in CUR@L was released the fastest, reaching more than 30%.

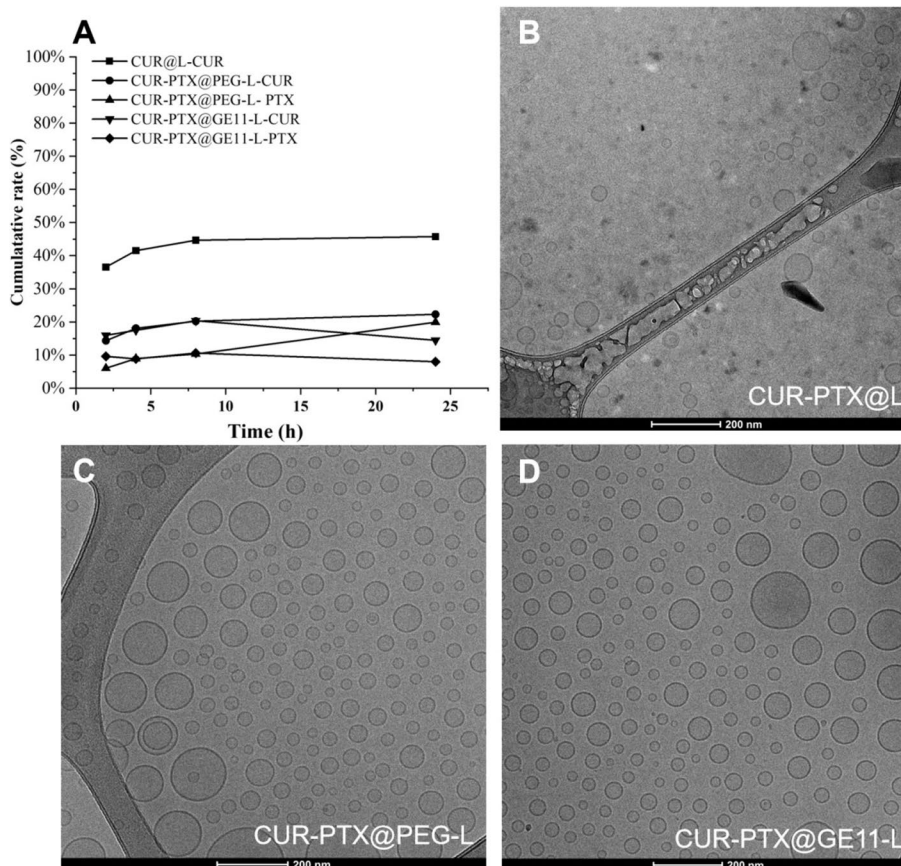


Fig. 1 **A** The in vitro release rate of CUR and PTX encapsulated in CUR@L, CUR-PTX@PEG-L, and CUR-PTX@GE11-L. **B–D** The morphology observation of CUR@L, CUR-PTX@PEG-L, and CUR-PTX@GE11-L by Cryo-TEM

Curcumin and paclitaxel were released relatively slowly in CUR-PTX@PEG-L and CUR-PTX@GE11-L. Curcumin was slightly higher than paclitaxel in the first 8 h of release but remained in the range of 10~20%, indicating that the drug release rate was obviously influenced by lipid prescription. This is different from the 50% ethanol release medium chosen for the RGD-modified CUR-PTX liposomes (Jiang et al. 2018), where pH7.4 PBS release medium was selected. Because both CUR and PTX are insoluble drugs, it is easy to reach a state of drug saturation during dialysis. In this experiment, the release medium reached the saturation state for CUR and PTX after 8 h release time.

Proliferation inhibition experiment of HUVEC

Human umbilical vein endothelial cells (HUVEC) were selected to observe the effects of different curcumin and paclitaxel liposome samples on cell proliferation and migration using a living cell workstation. As shown in Fig. 3, compared with PBS control group, the normal growth and proliferation of HUVEC were inhibited to varying degrees in the drug-containing group, resulting

in changes of cell morphology. Its effect was mainly manifested in the increase of the spacing between cells and the atrophy morphology of free extension and spreading of cells. The inhibition degree of cell growth and proliferation were obvious in the CUR@L group due to the high content of encapsulated curcumin and the fast drug release rate. In the CUR-PTX@PEG-L and CUR-PTX@GE11-L groups, although a few cells entering the G2 phase could be observed, the rate of division and proliferation became slow and remained G2-M stagnant for a long time. The inhibition effect of the drug-containing groups on cells depends more on the drug release rate of the preparations. CUR-PTX@GE11-L has no advantage over CUR@L mostly due to the slower encapsulated drug release, comparing to inefficient cell endocytosis.

The results of cell scratch trauma experiment showed that the drug-containing group could effectively inhibit cell proliferation and migration (Fig. 4). Among them, the CUR@L showed better inhibitory effect on cell migration. After drug administration, cells from the spread state into spheroid, the boundary between cells is clear. However, GE11-modified curcumin and

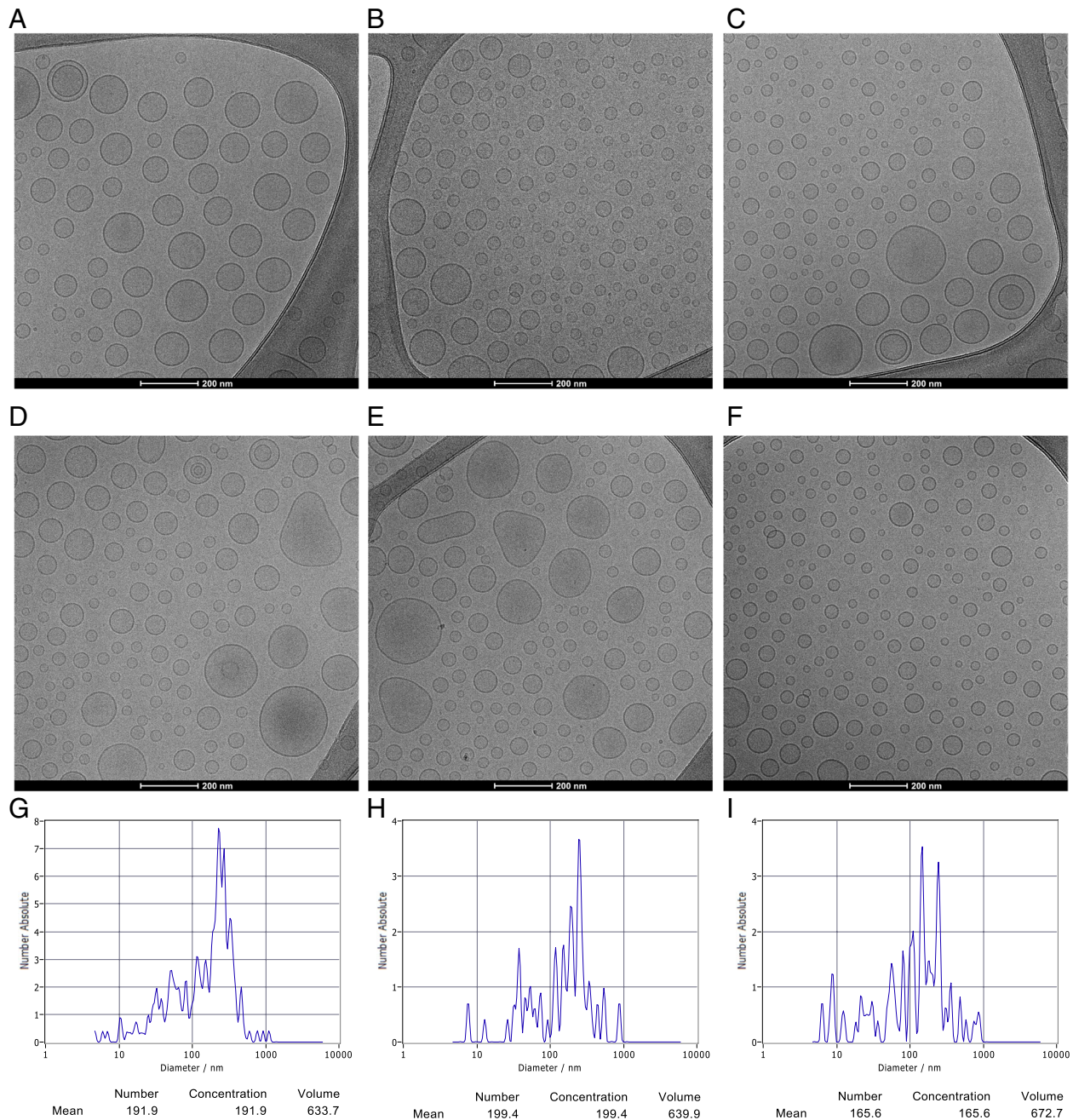


Fig. 2 A–C Cryo-TEM images of CUR-PTX@PEG-L. D–F Cryo-TEM images of CUR-PTX@GE11-L. G–I Signal particle tracking technology for the determination of particle size distribution characteristics of CUR@L (G), CUR-PTX@PEG-L (H), and CUR-PTX@GE11-L (I)

Table 2 The portion of irregular and multilayer liposomes prepared by microfluidic chip technology

	Total number	Irregular	Multilayer
CUR@L	200	1 (0.05%)	2 (0.1%)
CUR-PTX@PEG-L	300	0	5 (1.6%)
CUR-PTX@GE11-L	300	6 (2%)	0

paclitaxel liposomes did not show the advantage of cell migration inhibition, when comparing to CUR@L. As an EGFR-targeting nanoparticles, the cellular endocytosis of CUR-PTX@GE11-L can be influenced by the EGFR surface expression level of targeting cells. Therefore, rapid curcumin and paclitaxel release combined with the increase of cellular endocytosis of curcumin and paclitaxel compound liposome in the targeted

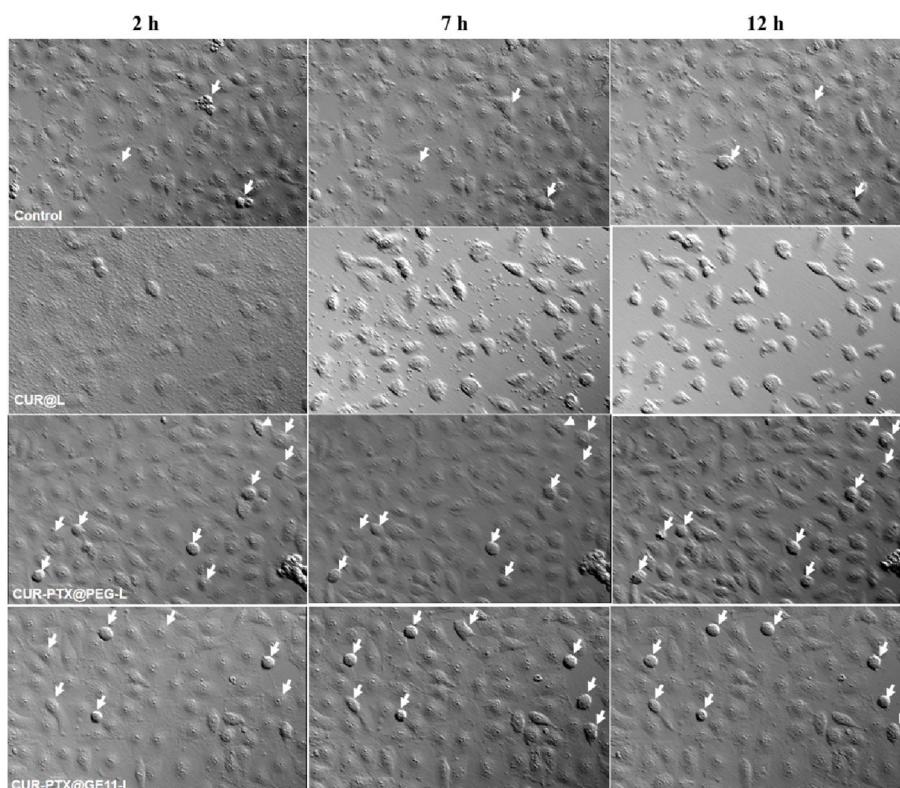


Fig. 3 Inhibition effect of CUR @L, CUR-PTX@PEG-L, and CUR-PTX@GE11-L on the proliferation of HUVEC cells observed by living cell workstation (12 h after administration)

tumor sites can promote synergistic therapeutic effects and cause the morphology changes of targeting cells, resulting in the spatial structure reconstitution of the tumor microenvironment. This also means that the rapid release of the loading drug at the targeting site combined with the high rate of endocytosis by the tumor cells can achieve the best cytotoxic efficacy.

Morphology changes of bone marrow stem cells (BMSCs)

BMSC are bone marrow derived mesenchymal stem cells. It has been documented that BMSC promote proliferation and invasion of HepG2 liver cancer cells (Mi and Gong 2017). The BMSC was stained with calcein after administration of curcumin and paclitaxel liposomes. The changes of BMSC morphology were observed. As shown in Fig. 5, BMSC cells in the control group had a large spread surface and were in a free stretch state, while for the drug administration group, the cell size tended to be decreased and showed a polycondensation state. The cell morphology and size dimension of CUR-PTX@GE11-L-treated group changed the most, followed by PTX@L, CUR-PTX@PEG-L, and CUR@L.

Targeting efficiency of CUR-PTX@GE11-L in SMMC7721 subcutaneous xenografts

The distribution of CUR-PTX@GE11-L in vivo in the SMMC7721 subcutaneous xenografts was observed by in vivo imaging system after administration of CUR-PTX@GE11-L every 3 days for three times (Fig. 6). CUR-PTX@GE11-L has obvious EGFR-overexpressed tumor targeting, which also has been confirmed in previous studies (Cheng et al. 2014). The liver, spleen, and lungs retained the high concentrations of CUR-PTX@GE11-L, especially the liver. The accumulation of CUR-PTX@GE11-L and CUR-PTX@PEG-L was observed in the foot and brain of mice, which confirmed the reason why paclitaxel is prone to neurotoxicity.

Discussion

Curcumin and paclitaxel have been widely studied as anti-tumor chemotherapy drugs. The two drugs can affect the growth and proliferation of tumor cells by acting on different signaling pathways, and their synergistic antitumor effect has been widely recognized (Vemuri et al. 2022). However, because curcumin and paclitaxel are both hydrophobic drug molecules, their

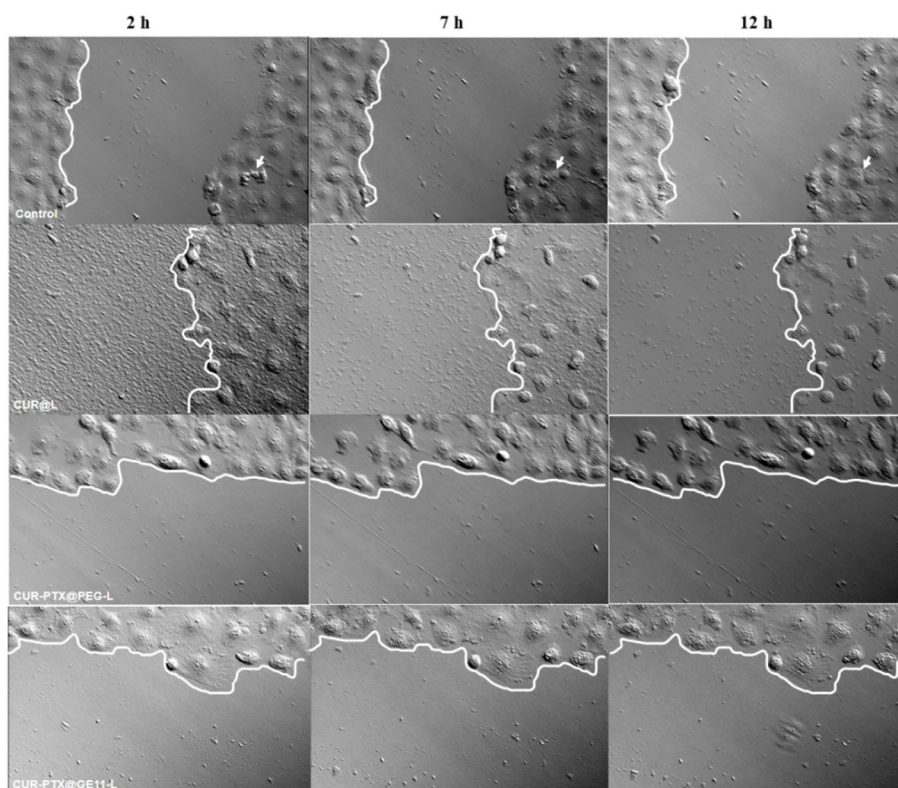


Fig. 4 Inhibition of CUR@L, CUR-PTX@PEG-L, and CUR-PTX@GE11-L on the migration of HUVEC cells observed by living cell workstation (12 h after administration)

bioavailability *in vivo* is greatly affected by drug solubility (Alemi et al. 2018).

In order to strengthen the therapeutic efficacy and targeting accumulation of the drugs, different novel nano-preparations are designed for specific tumor tissue targeting delivery of curcumin and paclitaxel (Xiong et al. 2020). Because of the high interstitial pressure in tumor tissues, it is very difficult for nanomaterials to penetrate into tumor tissue (Tang et al. 2020; Khawar et al. 2015). Thus, a variety of environmentally responsive intelligent nanomaterials are synthesized and successfully infiltrated into tissues (Zhu et al. 2019). However, there are few studies on the actions of curcumin and paclitaxel nano-preparations on tumor tissue interstitial cells and the way to increase permeability of tumor tissues based on cellular morphology changes (Boccellino et al. 2022).

In previous research work, it has been fully verified that GE11, EGFR-targeting dodecapeptide, can obviously improve the binding efficiency of GE11-modified nanoparticles with EGFR over-expressed tumor cells (Tang et al. 2014, 2020). A detailed experimental verification of GE11-modified doxorubicin liposomes was conducted to describe the mesenchymal barrier and receptor binding barrier at the targeting site. How to achieve the

targeting aggregation at the desired lesions and control drug release at the desired rate is the most key question involved in the designation of novel active-targeting nano-preparation (Hailing et al. 2022).

In this paper, paclitaxel and curcumin were selected as compound drugs loaded into liposomes, and we also observed the antitumor mechanism of paclitaxel and curcumin liposomes by imaging. The *in vitro* release features of encapsulated drugs from CUR-PTX@GE11-L were initially investigated. When EPC and cholesterol were consistent in PEG/GE11-modified liposome samples, the percentage of DSPE-MPEG and DSPE-MPEG-GE11 affected the release rate of encapsulated drugs. There is also a significant difference on the aspect of liposomal drug release behavior between CUR-PTX@GE11-L and CUR@L.

For the *in vitro* release study of paclitaxel and curcumin compound liposomes, a PBS buffer system with pH 7.4 was chosen as the release medium. The release of paclitaxel and curcumin at different pH conditions (such as pH 6.6 and pH 5.4) has not been carried out, mainly based on the fact that liposomes are first exposed to pH-neutral solution systems in cytotoxicity experiments and *in vivo* targeted efficiency studies. In order to better understand the release degree of paclitaxel and curcumin

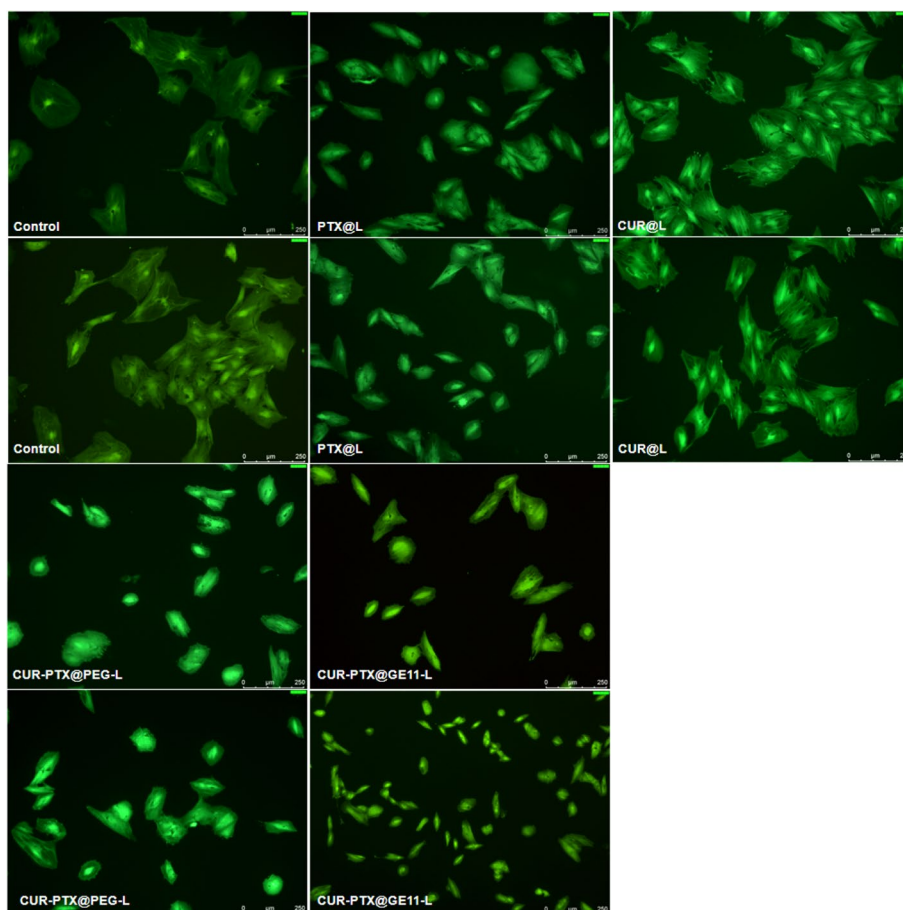


Fig. 5 Effects of different curcumin and paclitaxel liposome samples on the morphology change of BMSC (24 h after administration, bar = 250 μm)

compound liposomes in the acidic tumor microenvironment, it is also necessary to compare the different release behavior under different pH conditions in future study.

HUVEC is a kind of vascular endothelial cell. In this paper, through the cell proliferation and migration experiment, it is visually observed that HUVEC would atrophy and cell proliferation would stay at G2-M stage, after administration of CUR-PTX@GE11-L, but inferior to the significant changes in cell morphology that CUR@L brings about. This may be due to the fact that plane liposome can enter the cell through more pathways, including fusion, endocytosis, and pinocytosis (Dunham et al. 1977). BMSC cells are more significantly affected by CUR-PTX@GE11-L than CUR@L because the cell atrophy is more obvious. Both HUVEC and BMSC can act as tumor stromal cells and have an obvious effect on tumor angiogenesis and metastasis (Wang et al. 2019a, b; Zhang et al. 2019). Ding-Li Yu et al. have made a very detailed comparative retrospective analysis of the effects of paclitaxel on various tumor stromal cells (Yu et al. 2022). Due to the higher curcumin loading and faster release rate,

CUR@L had a more significant effect on the cell morphology of HUVEC selectively, while CUR-PTX@GE11-L make MDSC shrinkage more obviously, which could promote the penetration of liposome into tumor tissues.

EGFR expression level in tumor mesenchymal cells affects the endocytosis uptake of CUR-PTX@GE11-L (Cheng et al. 2014). Unlike EGF, GE11 does not effectively promote cell mitosis when combined with EGFR (Müller-Deubert et al. 2017; Schäfer et al. 2011). Liver tissue, as a natural aggregation organ of passive targeting of many nanoparticles, is the major site of drug adverse reactions. Previous studies have observed obvious aggregation at tumor sites after IV administration of GE11-modified nanoparticles (Cheng et al. 2014).

In this study, the accelerated accumulation phenomenon (AAP) of liposomes was taken into account (Wang et al. 2015; Yang et al. 2013). DID-labeled CUR-PTX@GE11-L and CUR-PTX@PEG-L were injected for three consecutive injections every 3 days to observe the elimination of the targeting efficiency due to AAP effect.

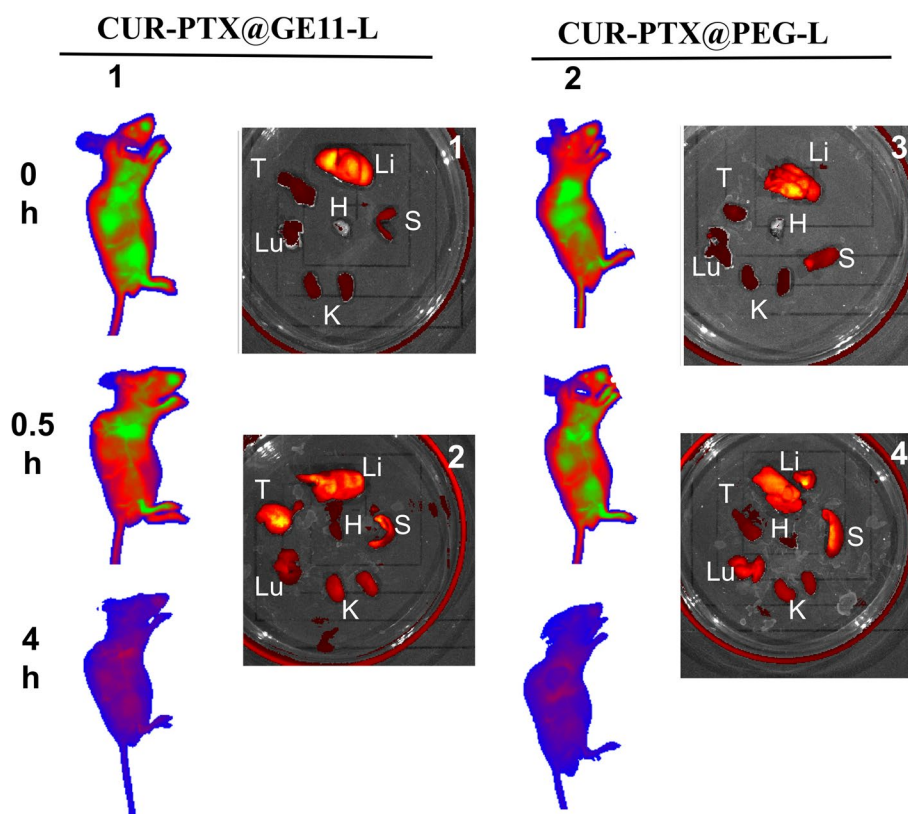


Fig. 6 Observation of the in vivo distribution of CUR-PTX@GE11-L and CUR-PTX@PEG-L in SMMC7721 subcutaneous xenografts at 4 h after administration and the tissue fluorescence strength at 24 h after sacrifice

IVIS imaging results exhibited nano-preparations which are difficult to escape and often retained in the liver, spleen, and lung organs after administration. The mice treated with CUR-PTX@GE11-L developed various degrees of hepatitis and liver injury, though many researchers described the hepatic protection from curcumin (Afrin et al. 2017). EGFR-targeting CUR-PTX@GE11-L can strengthen the penetration efficiency of nanoparticles into tumor microenvironment.

Most intelligent active targeting nano-preparations tend to choose the specific enzymatic response in the tumor microenvironment or employ light, heat, and magnet to achieve specific drug release at the target site (Lee and Thompson 2017). However, little literature focus on the effect of morphology change of tumor stromal cells on the targeting efficiency and penetration efficiency of nano-preparations. Up to now, there are still many challenges need to be overcome in the design of curcumin and paclitaxel active-targeted “smart” liposomes.

Conclusions

Numerous studies have been conducted extensively on the synergistic therapeutic effects of curcumin and paclitaxel on tumor cell signaling pathways. Here, the cellular morphology changes of tumor mesenchymal cells were focused. Imaging technology makes it feasibility to further understand the possibility of cell morphology changes to promote intra-tumoral penetration of targeted agents. It provides a novel meaningful manner for the design of anti-tumor intelligent targeting nano-agents, especially for the cytotoxic drug combination therapy.

Abbreviations

EGFR	Epidermal growth factor receptor
CUR	Curcumin
PTX	Paclitaxel
HUVEC	Human umbilical vein endothelial cells
TEM	Transmission electron microscopy
BMSC	Bone marrow stem cells

Acknowledgements

Not applicable.

Authors' contributions

Hailing Tang, Lijuan Li, and Baoshan Wang attended collecting the experimental resources and analyzed the experiment data, and Hailing Tang was the major contributor in writing and revising the manuscript. All authors read and approved the final manuscript.

Funding

Not applicable.

Availability of data and materials

All data generated during this study are included in this published article and can be made available on request.

Declarations**Competing interests**

The authors declare that they have no competing interests.

Author details

¹Guangxi University of Chinese Medicine Nanning, No.13 Wuhe Road, Qingxiu Area, Nanning, Guangxi 530200, China. ²Key Laboratory of Research and Development of Generic Technology of Traditional Chinese Medicine Preparations in Guangxi Universities, Nanning 530200, China. ³Qingdao Hospital of Traditional Chinese Medicine, Qingdao 266033, China. ⁴Department of Orthopaedics, Qilu Hospital (Qingdao), Cheeloo College of Medicine, ShanDong University, Qingdao 266035, China. ⁵Guangxi Scientific Research Center of Traditional Chinese Medicine, Guangxi University of Chinese Medicine, Nanning 530200, China.

Received: 16 March 2023 Accepted: 19 December 2023

Published online: 08 February 2024

References

- Afrin R et al (2017) Curcumin ameliorates liver damage and progression of NASH in NASH-HCC mouse model possibly by modulating HMGB1-NF- κ B translocation. *Int Immunopharmacol* 44:174–182
- Aggarwal BB et al (2005) Curcumin suppresses the paclitaxel-induced nuclear factor-kappaB pathway in breast cancer cells and inhibits lung metastasis of human breast cancer in nude mice. *Clin Cancer Res* 11(20):7490–7498
- Alemi A et al (2018) Paclitaxel and curcumin coadministration in novel cationic PEGylated niosomal formulations exhibit enhanced synergistic antitumor efficacy. *J Nanobiotechnol* 16(1):28
- Ashrafizadeh M et al (2020) Curcumin in cancer therapy: a novel adjunct for combination chemotherapy with paclitaxel and alleviation of its adverse effects. *Life Sci* 256:117984
- Barenholz Y (2012) Doxil[®]—the first FDA-approved nano-drug: lessons learned. *J Control Release* 160(2):117–134
- Blair HA (2018) Daunorubicin/cytarabine liposome: a review in acute myeloid leukaemia. *Drugs* 78(18):1903–1910
- Boccellino M et al (2022) The role of curcumin in prostate cancer cells and derived spheroids. *Cancers (Basel)* 14(14):3348
- Caillaud M et al (2022) Formulated curcumin prevents paclitaxel-induced peripheral neuropathy through reduction in neuroinflammation by modulation of α 7 nicotinic acetylcholine receptors. *Pharmaceutics* 14(6):1296
- Cheng L et al (2014) GE11-modified liposomes for non-small cell lung cancer targeting: preparation, ex vitro and in vivo evaluation. *Int J Nanomed* 9:921–935
- Cortes JE et al (2022) Efficacy and safety of CPX-351 versus 7 + 3 chemotherapy by European LeukemiaNet 2017 risk subgroups in older adults with newly diagnosed, high-risk/secondary AML: post hoc analysis of a randomized, phase 3 trial. *J Hematol Oncol* 15(1):155
- Dang YP et al (2015) Curcumin improves the paclitaxel-induced apoptosis of HPV-positive human cervical cancer cells via the NF- κ B-p53-caspase-3 pathway. *Exp Ther Med* 9(4):1470–1476
- Dunham P et al (1977) Membrane fusion: studies with a calcium-sensitive dye, arsenazo III, in liposomes. *Proc Natl Acad Sci U S A* 74(4):1580–1584
- El-Saadony MT et al (2022) Impacts of turmeric and its principal bioactive curcumin on human health: pharmaceutical, medicinal, and food applications: a comprehensive review. *Front Nutr* 9:1040259
- Gao H, He Q (2014) The interaction of nanoparticles with plasma proteins and the consequent influence on nanoparticles behavior. *Expert Opin Drug Deliv* 11(3):409–420
- Gur C et al (2022) Chemopreventive effects of hesperidin against paclitaxel-induced hepatotoxicity and nephrotoxicity via amendment of Nrf2/HO-1 and caspase-3/Bax/Bcl-2 signaling pathways. *Chem Biol Interact* 365:110073
- Hailing T et al (2022) Challenges for the application of EGFR-targeting peptide GE11 in tumor diagnosis and treatment. *J Control Release* 349:592–605
- Hamano N et al (2019) Robust microfluidic technology and new lipid composition for fabrication of curcumin-loaded liposomes: effect on the anticancer activity and safety of cisplatin. *Mol Pharm* 16(9):3957–3967
- Hailing T et al (2021) Optimization of compound liposome formulation of curcumin and paclitaxel by Box-Behnken response surface method. *Guangxi Univ Traditional Chin Med* 24(2):59–65
- Jiang K, Shen M, Xu W (2018) Arginine, glycine, aspartic acid peptide-modified paclitaxel and curcumin co-loaded liposome for the treatment of lung cancer: in vitro/vivo evaluation. *Int J Nanomedicine* 13:2561–2569
- Khaled SS et al (2022) The preventive effects of naringin and naringenin against paclitaxel-induced nephrotoxicity and cardiotoxicity in male Wistar rats. *Evid Based Complement Alternat Med* 2022:8739815
- Khawar IA, Kim JH, Kuh HJ (2015) Improving drug delivery to solid tumors: priming the tumor microenvironment. *J Control Release* 201:78–89
- Lee Y, Thompson DH (2017) Stimuli-responsive liposomes for drug delivery. *Wiley Interdiscip Rev Nanomed Nanobiotechnol* 9(5):e1450
- Liu Z et al (2016) Evaluation of the efficacy of paclitaxel with curcumin combination in ovarian cancer cells. *Oncol Lett* 12(5):3944–3948
- Liu Y et al (2022) Curcumin enhances the anti-cancer efficacy of paclitaxel in ovarian cancer by regulating the miR-9-5p/BRC1A1 axis. *Front Pharmacol* 13:1014933
- Mi F, Gong L (2017) Secretion of interleukin-6 by bone marrow mesenchymal stem cells promotes metastasis in hepatocellular carcinoma. *Biosci Rep* 37(4):BSR20170181
- Müller-Deubert S et al (2017) Epidermal growth factor as a mechanosensitizer in human bone marrow stromal cells. *Stem Cell Res* 24:69–76
- Muthoosamy K et al (2016) Exceedingly higher co-loading of curcumin and paclitaxel onto polymer-functionalized reduced graphene oxide for highly potent synergistic anticancer treatment. *Sci Rep* 6:32808
- Saghatelyan T et al (2020) Efficacy and safety of curcumin in combination with paclitaxel in patients with advanced, metastatic breast cancer: a comparative, randomized, double-blind, placebo-controlled clinical trial. *Phytomedicine* 70:153218
- Schäfer A et al (2011) Disconnecting the Yin and Yang relation of epidermal growth factor receptor (EGFR)-mediated delivery: a fully synthetic, EGFR-targeted gene transfer system avoiding receptor activation. *Hum Gene Ther* 22(12):1463–1473
- Tang H et al (2014) Effects of surface displayed targeting ligand GE11 on liposome distribution and extravasation in tumor. *Mol Pharm* 11(10):3242–3250
- Tang H et al (2020) Reimaging biological barriers affecting distribution and extravasation of PEG/peptide-modified liposomes in xenograft SMMC7721 Tumor. *Acta Pharm Sinica B* 10(3):546–556
- Vemuri SK et al (2022) Modulatory effects of biosynthesized gold nanoparticles conjugated with curcumin and paclitaxel on tumorigenesis and metastatic pathways-in vitro and in vivo studies. *Int J Mol Sci* 23(4):2150
- Wang C et al (2015) Accelerated blood clearance phenomenon upon cross-administration of PEGylated nanocarriers in beagle dogs. *Int J Nanomedicine* 10:3533–3545
- Wang J et al (2016) A multifunctional poly(curcumin) nanomedicine for dual-modal targeted delivery, intracellular responsive release, dual-drug treatment and imaging of multidrug resistant cancer cells. *J Mater Chem B* 4(17):2954–2962

- Wang N, Chen M, Wang T (2019a) Liposomes used as a vaccine adjuvant-delivery system: from basics to clinical immunization. *J Control Release* 303:130–150
- Wang Y et al (2019b) Extracellular vesicles (EVs) from lung adenocarcinoma cells promote human umbilical vein endothelial cell (HUVEC) angiogenesis through yes kinase-associated protein (YAP) transport. *Int J Biol Sci* 15(10):2110–2118
- Xiong K et al (2020) Co-delivery of paclitaxel and curcumin by biodegradable polymeric nanoparticles for breast cancer chemotherapy. *Int J Pharm* 589:119875
- Yamamoto HY, Bangham AD (1978) Carotenoid organization in membranes. Thermal transition and spectral properties of carotenoid-containing liposomes. *Biochim Biophys Acta* 507(1):119–127
- Yang Q et al (2013) Accelerated drug release and clearance of PEGylated epirubicin liposomes following repeated injections: a new challenge for sequential low-dose chemotherapy. *Int J Nanomedicine* 8:1257–1268
- Yu DL et al (2022) The interactions of paclitaxel with tumour microenvironment. *Int Immunopharmacol* 105:108555
- Zhang X et al (2019) Hypoxic BMSC-derived exosomal miRNAs promote metastasis of lung cancer cells via STAT3-induced EMT. *Mol Cancer* 18(1):40
- Zhang W et al (2022) Nanoparticle albumin-bound paclitaxel is superior to liposomal paclitaxel in the neoadjuvant treatment of breast cancer. *Nanomed (Lond)* 17(10):683–694
- Zhu F et al (2019) Smart nanoplatform for sequential drug release and enhanced chemo-thermal effect of dual drug loaded gold nanorod vesicles for cancer therapy. *J Nanobiotechnol* 17(1):44

Publisher's Note

Springer Nature remains neutral with regard to jurisdictional claims in published maps and institutional affiliations.